

23. I. Bezprozvanny, B. E. Ehrlich, *Neuron* **10**, 1175 (1993).
24. I. Bezprozvanny, B. E. Ehrlich, *J. Gen. Physiol.* **104**, 821 (1994).
25. I. C. B. Marshall, C. W. Taylor, *Biochem. J.* **301**, 591 (1994).
26. D. B. van Rossum *et al.*, *Proc. Natl. Acad. Sci. U.S.A.* **101**, 2323 (2004).
27. G. G. Du, D. H. MacLennan, *J. Biol. Chem.* **273**, 31867 (1998).
28. Y. Sekine-Aizawa, R. L. Huganir, *Proc. Natl. Acad. Sci. U.S.A.* **101**, 17114 (2004).
29. R. E. Dalbey, G. Von Heijne, *Protein Targeting, Transport, and Translocation* (Academic Press, San Diego, 2002).
30. We thank S. Lummis (Cambridge) for use of her Flexstation and T. Kurosaki (Kansai Medical University Japan) for providing DT40 cells. Supported by the Wellcome Trust (072084), Biotechnology and Biological Sciences Research Council, and a Jameel Family Studentship (to T-U-R).

## Supporting Online Material

www.sciencemag.org/cgi/content/full/313/5784/229/DC1

Materials and Methods

Figs. S1 to S7

Tables S1 to S3

References

20 January 2006; accepted 24 May 2006

10.1126/science.1125203

# Biomining of Gold: Biofilms on Bacterioform Gold

Frank Reith,<sup>1,2\*</sup> Stephen L. Rogers,<sup>1,4</sup> D. C. McPhail,<sup>1,2</sup> Daryl Webb<sup>3</sup>

Bacterial biofilms are associated with secondary gold grains from two sites in Australia. 16S ribosomal DNA clones of the genus *Ralstonia* that bear 99% similarity to the bacterium *Ralstonia metallidurans*—shown to precipitate gold from aqueous gold(III) tetrachloride—were present on all DNA-positive gold grains but were not detected in the surrounding soils. These results provide evidence for the bacterial contribution to the authigenic formation of secondary bacterioform gold grains and nuggets.

The origin of secondary gold grains is controversial and widely debated in the scientific community; the two main theories are that they are detrital or are formed by

chemical accretion (1). However, there is growing evidence pointing to the importance of microbial processes in the cycling of gold (2, 3). Common soil bacteria (*Bacillus megaterium*,

*Pseudomonas fluorescens*, *Bacterium nitrificans*) are able to solubilize several milligrams of gold per liter of medium under in vitro conditions (2, 4). A recent microcosm study of auriferous soils from the Tomakin Park Gold Mine in southeastern New South Wales, Australia (35°48'51.9"S, 150°10'26.4"E) showed that resident microbiota solubilized up to 80 wt % [i.e., 1100 ng per g (dry weight, soil)] of

<sup>1</sup>Cooperative Research Centre for Landscape Environments and Mineral Exploration, Post Office Box 1130, Bentley, Western Australia 6102, Australia. <sup>2</sup>Department of Earth and Marine Sciences, <sup>3</sup>Research School of Biological Sciences, Electron Microscopy Unit, Australian National University, Acton, ACT 0200, Australia. <sup>4</sup>Commonwealth Scientific and Industrial Research Organisation (CSIRO) Land and Water, PMB2, Glen Osmond, South Australia 5064, Australia.

\*To whom correspondence should be addressed. E-mail: frank.reith@csiro.au

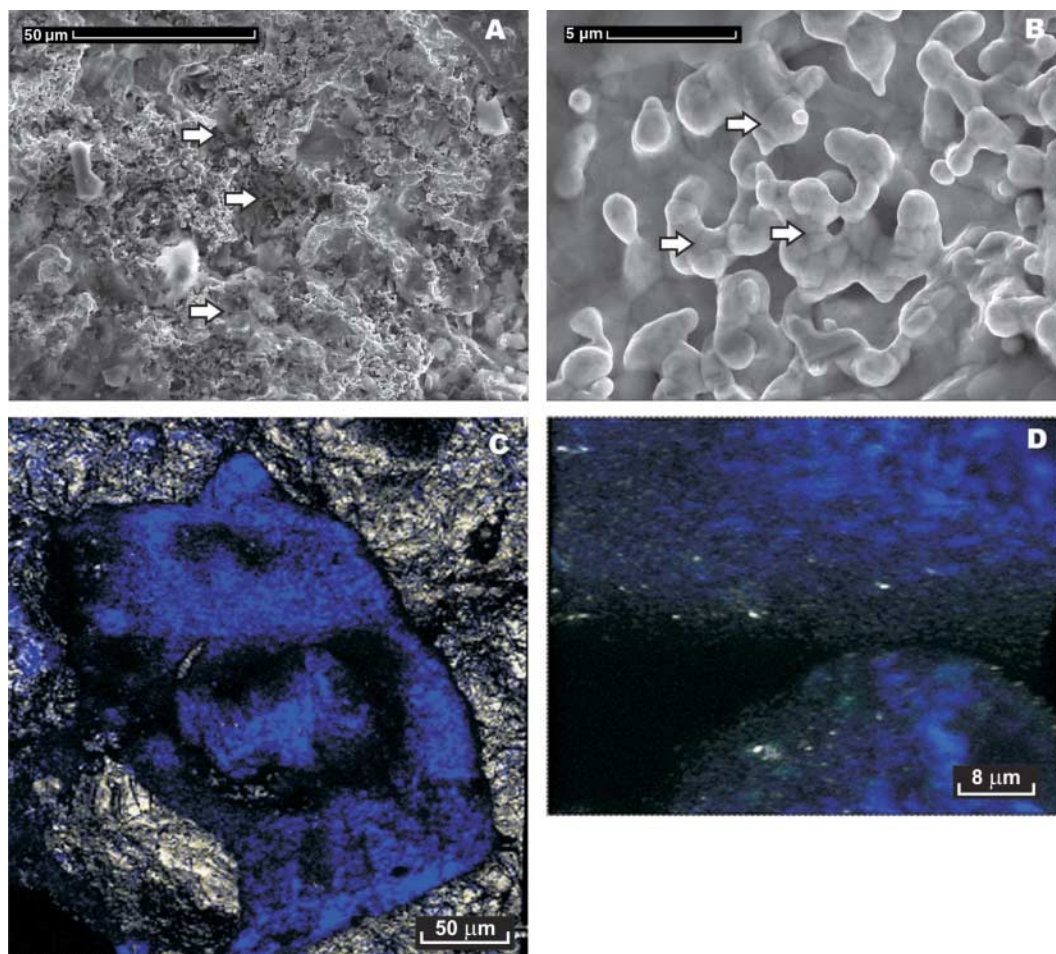


**Fig. 1.** Secondary electron micrographs of bacterioform gold (A and B) and confocal stereo laser microscope images (C and D) of fluorescently stained biofilms on gold grains from the Hit or Miss Gold Mine in Queensland, Australia. (A) Bacterioform gold with apparent exopolymers (white arrows) possibly derived from a microbial biofilm. (B) Detailed view of branching network of rounded and oval budding cell-like structure with apparently preserved cell wall structures (white arrows). (C) Biofilm covering an area of 200 µm by 100 µm of underlying bacterioform gold. (D) Detailed view into a small crevice in the biofilm, showing cells or cell clusters (in blue) separated by unstained interstices. Fluorescent cells are spreading predominantly over the surface of the bacterioform gold and are not present at the base of the crevice.

native gold within 45 days of incubation (5). In other studies, bacteria, actinomycetes, archaea, and fungi have been shown to precipitate Au(I/III) complexes under a wide range of experimental conditions (6–13). For example, *Bacillus subtilis* and *Pseudomonas aeruginosa* precipitate gold colloids intracellularly and extracellularly from  $\text{AuCl}_4^-$  solutions (8, 9). Lengke and Southam (11) have shown active intracellular precipitation of gold particles from  $\text{Au}(\text{S}_2\text{O}_3)_2^{3-}$  by *Acidithiobacillus thiooxidans*; they observed irregular, rounded gold particles and octahedral gold crystals that formed several months after bacterial growth had stopped. In field studies, structures resembling gold-encrusted microfossils observed on numerous gold grains from the Americas and Australia have suggested that microbial processes contribute to the formation of secondary gold grains (14–18). However, after producing similar structures with natural and artificial gold amalgams by hot nitric acid dissolution, Watterson and others concluded that the observed morphologies alone could not be considered adequate proof of the microbial origin of these grains (19, 20). Thus, the evidence to date for an association of bacteria with gold grains and their contribution to the formation of secondary grains is at best equivocal.

Gold grains for this study were obtained from soils overlying the mineralized zones at the Tomakin Park Gold Mine and the Hit or Miss Gold Mine, the latter of which is located

in tropical northern Queensland, Australia ( $16^\circ 03' 32''\text{S}$ ,  $144^\circ 19' 09''\text{E}$ ). Primary mineralization at both sites is submicroscopic and is associated with arsenopyrite and pyrite hosted in quartz (21, 22). In soils overlying mineralized zones, secondary gold grains (99.2 wt % fineness; table S1) ranging in size from 0.1 to 2.5 mm were obtained (fig. S1). These findings indicate that gold dissolution from the host material, transport of gold [possibly as  $\text{Au}(\text{I/III})$ -organic complexes or colloids], and accumulation and secondary gold grain formation had occurred in the weathering zone (23).

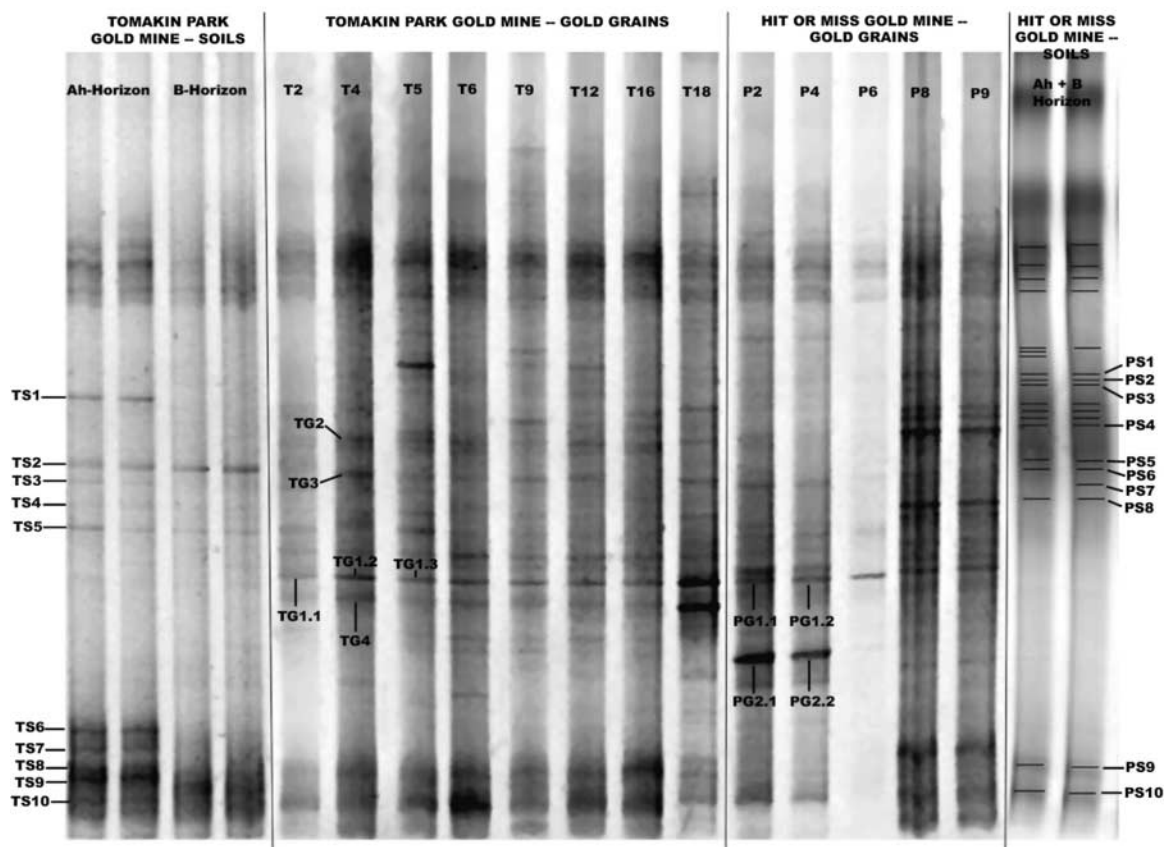
Scanning electron microscopy (SEM) of gold grains revealed micrometer-sized bacterioform pseudomorphs (Fig. 1, A and B) (23). Bacterial pseudomorphs detected on 5 of 10 grains from Tomakin Park Gold Mine and 7 of 10 from the Hit or Miss Gold Mine were spheroidal, cell-like structures with seemingly conserved cell walls (Fig. 1, A and B). Dried organic matter was observed in areas of bacterioform gold centered on surfaces of several grains (Fig. 1A) by means of SEM combined with spot energy-dispersive x-ray (EDX) analysis that showed carbon, oxygen, and nitrogen (fig. S2) (23). It is thus likely that the observed organic matter originated from extracellular polymeric substances of bacterial biofilms. Nucleic acid staining with 4',6'-diamidino-2-phenylindole (DAPI) combined with confocal stereo laser microscopy confirmed the presence of extensive biofilms on gold grains covered with

bacterial pseudomorphs (Fig. 1, C and D) (23). High-resolution imagery showed an uneven distribution of DAPI within the biofilm, indicating staining of nucleic acids within individual cells (Fig. 1D), whereas zones without cellular structures did not stain positive with DAPI.

Twenty gold grains from each site were used as templates for polymerase chain reactions, and 16S ribosomal DNA (rDNA) was amplified from 80% of these grains (23). Denaturing gradient gel electrophoresis (DGGE) and SYBR-Gold (Invitrogen) staining were used to separate and visualize the 16S rDNA bands, respectively (23). The number of detected bands points to the presence of up to 30 different bacterial species on the individual grains (Fig. 2). Analyses of DGGE fingerprints and 16S rDNA clone libraries of the bacterial communities associated with the bacterioform gold grains show that they are distinct and differ from those dominating the surrounding soils (Fig. 2 and table S2) (23). One 16S rDNA sequence was associated with all DNA-positive gold grains, irrespective of the site, but was not detected in the surrounding soils (Fig. 2). 16S rDNA clones from this band (TG1.1 to 1.3, PG1.1 and 1.2; Fig. 2) displayed 99% similarity to *Ralstonia metallidurans* (fig. S3 and table S2).

*R. metallidurans* is a Gram-negative, non-spore-forming  $\beta$ -proteobacterium that is highly resistant to metals, grows in the presence of

**Fig. 2.** DGGE patterns obtained after amplifying the V3 region of the 16S rDNA extracted from gold grains and surrounding soils collected at the Tomakin Park (T) and Hit or Miss (P) gold mines. Bands designated with acronyms were excised from the gels, reamplified, and sequenced. The banding of the Hit or Miss soil samples was visually enhanced with Adobe Photoshop.





millimolar concentrations of dissolved heavy metals such as Ag(I), Zn(II), Cd(II), Co(II), Pb(II), Hg(II), Ni(II), and Cr(VI), and has also been shown to reductively precipitate some of these metals [i.e., Ag(I), Cd(II), and Zn(II)] (24, 25). Thus, in a first set of experiments, the ability of *R. metallidurans* to precipitate gold by reducing soluble, toxic  $\text{AuCl}_4^-$  complexes was tested (23, 26). In an unamended growth medium, *R. metallidurans* multiplied exponentially for 16 hours from the start of the incubation before reaching a stationary phase, where viable cell numbers increased from the original inoculum of  $4.2 \times 10^4$  cells/ml to  $1.5 \times 10^8$  cells/ml (fig. S4) (23). In the growth medium amended with  $50 \mu\text{M}$   $\text{AuCl}_4^-$ , viable cell num-

bers declined to  $10^3$  cells/ml at 4 hours after inoculation and then increased to  $1.8 \times 10^7$  cells/ml after 72 hours (fig. S4). Initial gold precipitation by *R. metallidurans* was rapid, and after 8 hours of incubation, about  $3 \mu\text{M}$  gold had been precipitated. Subsequently, the precipitation of gold was slower, and at the end of the experiment, after 72 hours,  $5.5 \mu\text{M}$  gold had been precipitated (fig. S4). These results show that gold toxicity initially led to the death of more than 90% of viable cells from the original inoculum. The remaining cells were able to grow in the  $\text{AuCl}_4^-$ -amended medium, indicating that *R. metallidurans* harbors a resistance to  $\text{AuCl}_4^-$  toxicity and is able to adapt to high gold concentrations. In a second set of experiments,

the precipitation of gold by viable and lysed cells was assessed (23). Lysed, metabolically inactive *R. metallidurans* cells accumulated less than 50 wt % of gold relative to biologically active cells, indicating that *R. metallidurans* may be able to actively reduce  $\text{AuCl}_4^-$  and accumulate metallic gold (fig. S5).

Two types of gold accumulation, associated with viable *R. metallidurans* cells, were observed. *R. metallidurans* accumulated metallic gold in distinct areas on or just below the cell surface (Fig. 3A); three-dimensional SEM imaging and SEM-EDX spot analysis showed that cells precipitated metallic gold in distinct areas within the cells close to cell walls (Fig. 3B). Other *R. metallidurans* cells displayed no discrete areas of gold accumulation and appeared to be entirely covered by gold, which appeared to be associated with sulfur- and phosphorus-containing substances in the cell membrane or the cell wall (Fig. 3C).

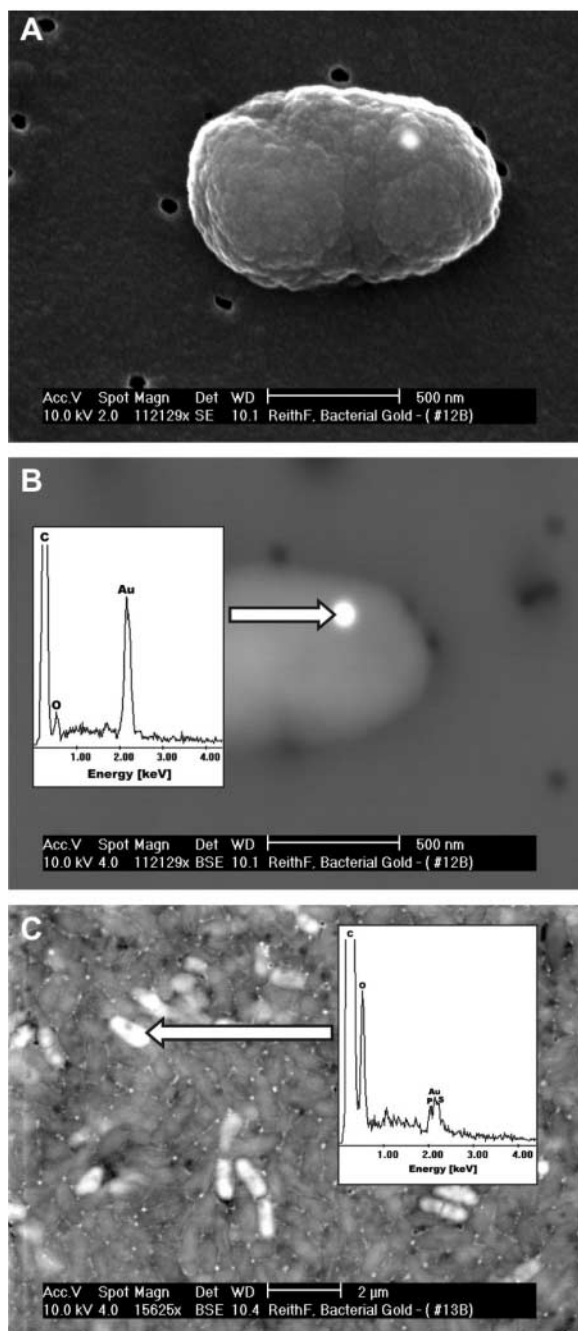
The biochemical mechanisms of gold precipitation in *R. metallidurans* are not yet understood. However, several mechanisms for heavy metal resistance have been observed in the organism, including cation efflux, cation reduction, cytoplasmic accumulation, and organic compound formation (24, 25). Energetic considerations, based on the mechanism for reductive precipitation of monovalent silver complexes, suggest that *R. metallidurans* prefers to reductively precipitate gold nanoparticles from  $\text{AuCl}_4^-$  in order to detoxify its immediate environment (25). Energy-dependent reductive precipitation of gold has been shown for other bacteria and archaea (10, 12, 13), and Lengke and Southam (11) have shown the intracellular precipitation of gold from  $\text{Au}(\text{S}_2\text{O}_3)_3^{3-}$  by *Acidithiobacillus thiooxidans*. Passive gold accumulation via sulfur- and phosphorus-containing molecules (such as the carboxylates and phosphates) present in the lipopolysaccharides in the cell walls of Gram-negative dead or live bacterial cells cannot be ruled out, and such a mechanism may explain the presence of cells that were entirely covered by gold.

This study provides evidence that bacterially mediated processes contribute to the formation of secondary gold grains. The dominant group of organisms identified, *Ralstonia* sp., may gain a metabolic advantage by living in areas of high gold toxicity in that it uses precipitation of toxic gold complexes as a biological detoxification mechanism. It can therefore be concluded that the structures described as bacterioform gold by previous authors may indeed be of bacterial origin.

#### References and Notes

1. R. W. Boyle, *Geol. Surv. Can. Bull.* **280** (1979).
2. E. D. Korobushkina, G. I. Karavaiko, I. M. Korobushkin, in *Environmental Biogeochemistry*, R. Hallberg, Ed. (Publishing House of the Swedish Research Councils, Stockholm, 1983), vol. 35, pp. 325–333.
3. D. J. Mossman, T. Reimer, H. Durstling, *Geosci. Can.* **26**, 131 (1999).

**Fig. 3.** Secondary (A) and backscatter electron micrographs with spot EDX analysis (B and C) of *Ralstonia metallidurans* cells from experiments amended with  $50 \mu\text{M}$   $\text{AuCl}_4^-$  after 5 days of incubation at  $30^\circ\text{C}$  on a shaking incubator (100 rpm). Secondary (A) and backscatter (B) electron micrographs show a single *R. metallidurans* cell with colloidal metallic gold precipitate. Scale bar, 500 nm. (C) Backscatter electron micrograph of gold-covered *R. metallidurans* cells. Scale bar,  $2 \mu\text{m}$ .



4. N. N. Lyalikova, L. Y. Mockeicheva, *Microbiology* **38**, 682 (1969).
5. F. Reith, D. C. McPhail, *Geochim. Cosmochim. Acta* **70**, 1421 (2006).
6. V. I. Karamushka et al., *Prikl. Biokhim. Microbiol.* **23**, 697 (1987).
7. A. Nakjima, *World J. Microbiol. Biotechnol.* **19**, 369 (2003).
8. S. Karthikeyan, T. J. Beveridge, *Environ. Microbiol.* **4**, 667 (2002).
9. G. Southam, T. J. Beveridge, *Geochim. Cosmochim. Acta* **58**, 4227 (1994).
10. K. Kashefi, J. M. Tor, K. P. Nevin, D. Lovley, *Appl. Environ. Microbiol.* **67**, 3275 (2001).
11. M. Lengke, G. Southam, *Geochim. Cosmochim. Acta* **69**, 3759 (2005).
12. V. I. Karamushka, Z. R. Ulberg, T. G. Gruzina, *Ukr. Biokhim. Zh.* **62**, 76 (1990).
13. V. I. Karamushka, T. G. Gruzina, Z. R. Ulberg, *Ukr. Biokhim. Zh.* **62**, 103 (1990).
14. S. Mann, *Nature* **357**, 358 (1992).
15. J. R. Watterson, *Geology* **20**, 1147 (1992).
16. G. C. O. Bischoff, *N. Jb. Geol. Palaeont. Abh.* **194**, 187 (1994).
17. G. C. O. Bischoff, *N. Jb. Geol. Palaeont. Abh.* **H6**, 329 (1997).
18. J. L. Keeling, *South Australia Geol. Surv. Q. Geol. N.* **126**, 12 (1993).
19. J. R. Watterson, *Geology* **22**, 1144 (1994).
20. J. Erlebacher, M. J. Aziz, A. Karma, N. Dimitrov, K. Sieradzki, *Nature* **410**, 450 (2001).
21. H. N. Bowman, *A Brief Inspection of the Tomakin Park Gold Mine* (Geol. Surv. Rep. GS. 1979/256, Department of Mineral Resources and Development, Sydney, Australia, 1979).
22. R. J. Bultitude, P. J. T. Donchak, *Pre-Mesozoic Stratigraphy and Structure of the Maytown Region* (Queensland Resource Industries Record 1992/5, Department of Resource Industries, Brisbane, Australia, 1992).
23. See supporting material on Science Online.
24. Mergeay et al., *FEMS Microbiol. Rev.* **27**, 385 (2003).
25. M. L. Ledrich, S. Stemmler, P. Laval-Gilly, L. Foucaud, J. Falla, *Biomaterials* **18**, 643 (2005).
26. P. L. Witkiewicz, C. F. Shaw, *J. Chem. Soc. Chem. Commun.* **21**, 1111 (1981).
27. We thank P. Wyatt, and K. Wyatt, and the Queensland Park and Wildlife Services for access to the sites; S. McClure and S. Welch for help with SEM and EDX analysis; and M. McLaughlin, E. Lombi, S. A. Wakelin, and G. Lawrence for reviewing the manuscript. Supported by grants from the Cooperative Research Centre for Landscape Environments and Mineral Exploration and by the Australasian Institute of Mining and Metallurgy (AusIMM).

# Supporting Online Material

www.sciencemag.org/cgi/content/full/313/5784/233/DC1  
Materials and Methods  
Tables S1 and S2  
Figs. S1 to S5  
References

6 February 2006; accepted 30 May 2006  
10.1126/science.1125878

## Selective Silencing of Foreign DNA with Low GC Content by the H-NS Protein in *Salmonella*

William Wiley Navarre,<sup>1</sup> Steffen Porwollik,<sup>4</sup> Yipeng Wang,<sup>4</sup> Michael McClelland,<sup>4</sup> Henry Rosen,<sup>2</sup> Stephen J. Libby,<sup>1\*</sup> Ferric C. Fang<sup>1,2,3,\*†</sup>

Horizontal gene transfer plays a major role in microbial evolution. However, newly acquired sequences can decrease fitness unless integrated into preexisting regulatory networks. We found that the histone-like nucleoid structuring protein (H-NS) selectively silences horizontally acquired genes by targeting sequences with GC content lower than the resident genome. Mutations in *hns* are lethal in *Salmonella* unless accompanied by compensatory mutations in other regulatory loci. Thus, H-NS provides a previously unrecognized mechanism of bacterial defense against foreign DNA, enabling the acquisition of DNA from exogenous sources while avoiding detrimental consequences from unregulated expression of newly acquired genes. Characteristic GCAT ratios of bacterial genomes may facilitate discrimination between a cell's own DNA and foreign DNA.

H-NS (encoded by *hns*) belongs to a family of small abundant nucleoid-associated proteins of Gram-negative bacteria that have the ability to bind DNA with relatively low sequence specificity (1). H-NS has been shown to act as a transcriptional repressor and can multimerize into higher order bridging complexes after DNA binding (1, 2). H-NS also affects local supercoiling, leading to the suggestion that H-NS and other nucleoid binding proteins represent the bacterial functional equivalent of histones or mediate the global modulation of gene expression in response to changes in temperature or osmolarity (1, 3, 4). H-NS has higher affinity for curved DNA, and no consensus sequence has been identified, al-

though the few H-NS binding sites mapped to date are rich in AT.

To determine the *Salmonella* genes controlled by H-NS, construction of an *hns* null mutation was attempted in *Salmonella enterica* sv. Typhimurium (*S. Typhimurium*). However, *hns* mutant strains were found to be nonviable unless additional mutations were present in either *rpoS* encoding the alternative sigma factor  $\sigma^S$  ( $\sigma^{32}$ ) or *phoP* encoding the virulence gene regulator PhoP. These mutants could tolerate an *hns* mutation but exhibited a reduced growth rate, whereas an *hns* mutation in an *rpoS phoP* double-mutant background displayed growth similar to that of the wild type (fig. S1). This suggests that the detrimental effect of an *hns* mutation is due to derepression of one or more  $\sigma^S$ - and PhoP-activated loci and might explain why *hns* mutations are not lethal in some laboratory strains, given that *rpoS* mutant alleles are commonly acquired after laboratory passage (5). To enable studies of H-NS function in *Salmonella*, we constructed an *hns* mutation in *S. Typhimurium* carrying a sponta-

neous *rpoS* mutation that confers diminished  $\sigma^S$  activity (6).

*Salmonella* genes regulated by H-NS were identified by comparing transcript levels in *hns*<sup>+</sup> and *hns*<sup>-</sup> strains by cDNA microarray analysis (Fig. 1 and table S1). Of 4529 open reading frames (ORFs) represented on the array (4422 from the chromosome and 107 from the virulence plasmid), transcript levels of 178 ORFs exhibited a reduction in abundance in the *hns* mutant to a level less than one-third that of the wild type, whereas 409 transcripts were more abundant in the *hns* mutant. As previously reported for *Escherichia coli*, many H-NS-activated genes are involved in chemotaxis and motility (7). Among genes repressed by H-NS are many known virulence loci of *Salmonella*, including the *Salmonella* pathogenicity island (SPI) 2, SPI-3, and SPI-5, most characterized virulence islets, and the plasmid *spv* genes.

A large number of H-NS-repressed genes bear the hallmarks of acquisition from a foreign source—i.e., they are not universally present in the genomes of closely related enteric bacteria and possess substantially reduced GC content compared with that of the resident genome (8). Of 409 ORFs exhibiting repression by H-NS, only 40 (9.8%) are common to all reference genomes, whereas 265 (64.7%) are found exclusively in *Salmonella* (table S1). Most H-NS-repressed genes have GC content that is lower than the overall genome: For ORFs in which H-NS was found to repress expression to one-third or less of the original level, the average GC content is 46.8%, whereas the average GC content of the entire *Salmonella* LT2 genome is 52.2% (Fig. 2A).

Microarray analysis of cDNA provides only indirect evidence that a transcription factor interacts directly with a given sequence, because many regulatory interactions are dependent on a cascade of transcription events. For example, the apparent activation of flagellar genes by H-NS most likely occurs by means of H-NS-mediated repression of *hdfR*, a repressor of the

<sup>1</sup>Department of Laboratory Medicine, <sup>2</sup>Department of Medicine, <sup>3</sup>Department of Microbiology, University of Washington, Seattle, WA 98195, USA. <sup>4</sup>Sidney Kimmel Cancer Center, San Diego, CA 92121, USA.

\*These authors contributed equally to this work.

†To whom correspondence should be addressed. E-mail: fcfang@u.washington.edu